Multiphase Image Segmentation Using the Deformable Simplicial Complex Method

Dahl, Vedrana Andersen; Christiansen, Asger Nyman; Bærentzen, Jakob Andreas

Published in:
Proceedings of 22nd International Conference on Pattern Recognition (ICPR 2014)

Link to article, DOI:
10.1109/ICPR.2014.182

Publication date:
2014

Document Version
Peer reviewed version

Multiphase Image Segmentation Using the Deformable Simplicial Complex Method

Vedrana Andersen Dahl
Asger Nyman Christiansen
Jakob Andreas Bærentzen
DTU Compute
Technical University of Denmark
{vand, asny, janba}@dtu.dk

***Abstract*—The deformable simplicial complex method is a generic method for tracking deformable interfaces. It provides explicit interface representation, topological adaptivity, and multiphase support. As such, the deformable simplicial complex method can readily be used for representing active contours in image segmentation based on deformable models. We show the benefits of using the deformable simplicial complex method for image segmentation by segmenting an image into a known number of segments characterized by distinct mean pixel intensities.**

I. Introduction

Segmentation is one of the basic operations in 2D as well as 3D image processing. In some cases, segmentation is performed by labeling pixels. However, often we wish to impose some geometric restrictions to the region being segmented, which can be done via a *deformable model*. In 2D, a deformable model is a curve that performs the segmentation by evolving under forces derived from the image. Such models are generally classified as either *explicit* (in the context of image segmentation also called parametric) or *implicit* (also called geometric), depending on the method used for representing the curve. Explicit methods utilize a parametric representation of the curve in a Lagrangian formulation, while implicit methods represent the curve as a level set of two dimensional function which evolves according to an Eulerian formulation. Despite this fundamental difference in curve representation, the underlying principles of both methods are the same [1].

Still, the choice of the curve representation is crucial for the implementation of the deformable model. The explicit methods represent curves accurately with a desired resolution. Furthermore, forces are applied directly to the curve. As a drawback, the explicit methods are prone to self-intersections and do not handle topology changes. For implicit methods the biggest benefit is a trivial support of topology changes during evolution. As a drawback, the implicit curve representation is bound to a regular grid. Moreover, it might be difficult to incorporate desired forces in an implicit formulation.

To develop an image segmenting framework which will not inherit the limitations of the underlying curve representation, we need a method which is explicit, yet supports topology changes. The deformable simplical complex (DSC) method developed by Misztal and Bærentzen [2] comes with those two important properties, and more. Apart from allowing for an explicit curve representation and robust topological adaptivity the DSC method has a natural multiphase support.

The DSC method is implemented in 2D and 3D, and has application in fluid simulation [3], [4], topology optimization [5] and computing cut loci on Riemannian manifolds [6]. In this paper we present an initial investigation in using 2D DSC for image segmentation. Our aim is to test the behaviour of the DSC method when coupled with image data, with focus on topological adaptivity and multiphase support. We consider an image, which is to be segmented into a known number of phases with distinctive mean pixel intensities. This is because we want to test the performance of the DSC based image segmentation in a well-known setting. For the same reason, we seek inspiration for the forces governing segmentation among the popular and well tested methods, which express the image segmentation problem in the formalism of deformable models, using either the explicit or the implicit representation of the curve. We bring an overview of such methods in the following section.

II. Background

The basic principle of deformable models is to perform image segmentation by evolving a curve in an image. The curve moves under the influence of *external forces*, which are computed from the image data, and *internal forces* which have to do with the curve itself. The popularity of deformable models is largely due to the well known snakes method by Kass et al. [7]. Snakes utilize an explicit curve representation $\mathbf{X}(s,t) = (x(s,t), y(s,t))$ where $s \in [0,1]$ is arclength and $t \in \mathbf{R}^+$ is time, which in a discrete setting reduces to a sequence of points. Such a curve evolves with external and internal forces

$$\frac{\partial \mathbf{X}}{\partial t} = \mathbf{F}_{\text{ext}}(\mathbf{X}) + \mathbf{F}_{\text{int}}(\mathbf{X})\,. \tag{1}$$

In the classical snakes formulation, the external forces are edge based and act by pulling the curve toward the image locations with a large gradient magnitude. The internal forces discourage stretching and bending of the curve segments,

$$\mathbf{F}_{\text{int}}(\mathbf{X}) = \frac{\partial}{\partial s}\left(\alpha \frac{\partial \mathbf{X}}{\partial s}\right) + \frac{\partial^2}{\partial s^2}\left(\beta \frac{\partial^2 \mathbf{X}}{\partial s^2}\right)\,, \tag{2}$$

with weights α and β controlling the elasticity and the rigidity term.

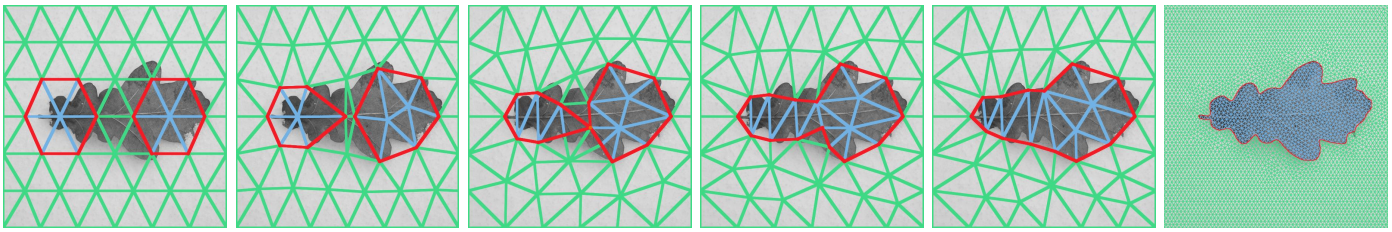

Fig. 1. An example of a coarse simplicial complex showing the topological adaptivity of the DSC method. Interface edges are displayed in red, edges between two *outside* triangles are green, and edges between two *inside* triangles are blue. As the interface deforms under segmentation forces, the topology automatically changes: the *inside* phase undergoes a merge while the *outside* phase undergoes a split. For comparison, the last image shows simplicial complex with a ten times smaller average edge length.

Following the success of snakes, an abundance of external forces has been proposed (see [8] for a comprehensive overview), most aiming at increasing the attraction range of external forces. The deformable models with an explicit curve representation have difficulties handling topology changes, such as merging or splitting. Whenever such a change occurs a costly reparametrization scheme is needed [9].

As the solution to the problem of topological adaptivity, the approaches utilizing implicit curve representation emerged [10], [11]. The curve is here represented as a zero level set of a 2D scalar function $\phi(x, y, t)$ defined on the image. The curve is evolved in accordance with a level set [12] equation

$$\frac{\partial \phi}{\partial t} = v(\kappa)|\nabla \phi|\,, \tag{3}$$

where $\nabla\phi$ denotes the gradient of ϕ, κ is the curvature at the zero level set and $v(\kappa)$ is a given speed function coupled with the image data. In the original formulation a speed function is constructed such that it vanishes in image locations with large gradient magnitude. The evolution will therefore stop when the curve meets an edge of the segmentation object.

The external forces described so far are edge based, which provides only a local support and is unsuitable for noisy images or when segmenting objects with weak edges. Region-based methods [13], [14] utilize a global information obtained from the curve to guide a segmentation. Those methods formulate a level set solution of Mumford-Shah [15] minimization problem seeking a piecewise smooth (or, as a reduced case, a piecewise constant) approximation of an image. The deforming forces depend not only on curve position but also on the current partitioning of the image. The level set equation for two-phase case (an object and a background) and without the term regularizing the length of the curve is

$$\begin{aligned} \frac{\partial \phi}{\partial t} &= \left[(I - m_{\text{in}})^2 - (I - m_{\text{out}})^2\right] |\nabla \phi| \\ &= (m_{\text{out}} - m_{\text{in}})(I - m_{\text{out}} + I - m_{\text{in}})|\nabla \phi|\,. \end{aligned} \tag{4}$$

Here m_{in} and m_{out} are current means of the area inside of the curve and outside of the curve, while $I(x, y)$ is used to denote the image. This speed function can be viewed as a signed pressure force, such that the curve shrinks where it is outside the object and expands where it is inside the object.

A common way of representing more than two phases is to employ more than one level set function. One solution is to represent each phase with one level set as in [16] where an additional energy is introduced to minimize (but not eliminate) overlap and vacuum. The regional based multiphase framework proposed in [17] uses a hierarchical approach with subsequent segmentation of previously obtained segments, allowing for an unknown number of phases, but having the limitation of segmenting all triple junctions as T-junctions. In [18] 2^n phases can be represented using n level sets by assigning a unique combination of n positive or negative signs to each phase, with the drawback of a possible bias where more than two phases meet.

Image segmentation using the DSC method complies fully with the formal framework of the deformable models. All forces suggested in this section, both in explicit and implicit formulation, can be applied to the curves represented with DSC. Furthermore, since DSC comes with a natural multiphase support it allows a multiphase segmentation without the tedious level set coupling.

III. Method

The DSC method is a key ingredient of our approach. Therefore, we start this section with a description of the principles and features of the DSC method with a focus on the 2D variant. The reader interested in implementational details or the 3D version is referred to work by Misztal and Bærentzen [2]. In the rest of this section we discuss the image segmentation forces applied to the DSC curve. Even though the DSC method provides a natural multiphase support, we first consider a two-phase case, which we later extend to cover a multiphase case.

A. The Deformable Simplicial Complex Method

Like the level set method, the DSC method is a method for dealing with deformable interfaces. While level sets are defined on a regular grid, the DSC is defined on a simplicial complex, corresponding to the triangularization of the 2D domain (tetrahedralization in 3D). Just as the sign of the level set function determines whether a grid point is inside or outside the curve, the triangles of DSC are labeled either *inside* or *outside* (in 3D the tetrahedra are labeled). As a result, a DSC interface is a curve (surface in 3D) composed of line segments (triangles in 3D) dividing interior from exterior, as illustrated in Fig. 1.

The deformation of the interface is performed by displacing the interface points. Consequently, the DSC method is explicit in nature and it preserves the advantages of Lagrangian methods, despite the described analogy with level sets. Still, the DSC method shares the biggest advantage

of the Eulerian methods – topological adaptivity. Whenever the interface moves, the triangulation (tetrahedralization) is updated to accommodate the change. If, for example, the two components collide, this change will cause them to merge (also shown in Fig. 1).

The key to this topological adaptivity lies in a series of mesh operations performed with each deformation of the interface. Loosely described, the procedure in the 2D case is as follows. Given a desired displacement of the interface, the interface points are not moved to their destination in a single step. Instead, each point is moved in the direction of the destination as far as possible *without* inverting triangles. When all points have moved, a mesh improvement routine is applied. This includes removing degenerate triangles, increasing the mesh quality (via Laplacian smoothing and edge flips) and inserting points. The interface points are then moved further toward their destination. This is repeated until all points have reached their destination. Mesh improvement routine relies on some chosen threshold values, e.g. defining when a triangle is degenerate. Those thresholds are a *part of* DSC. The only parameter required from a user is an average edge length of the triangles.

To summarize, the DSC method represents an interface in an explicit manner and yet it handles topology changes. Deformation of the interface is obtained by defining a displacement of vertices, possibly supplemented by actively changing labels of some triangles. And lastly, DSC has a natural multiphase support. One can use an arbitrary number of triangle labels rather than just *inside* and *outside*.

B. Two-Phase Segmentation

Our two-phase segmentation approach evolves a curve with external and internal forces. External forces are region-based and are directly adopted from (4), but explicitly formulated as forces acting on the curve points $\mathbf{X}$ as

$$\mathbf{F}_{\text{ext}}(\mathbf{X}) = (m_{\text{out}} - m_{\text{in}})(I - m_{\text{out}} + I - m_{\text{in}})\mathbf{N}\,, \qquad (5)$$

where $\mathbf{N}$ is an outward pointing normal.

For internal forces we use (2). It should be noted, however, that the first regulatory term (elasticity) has a different role here than in classical snakes, where it holds the curve points close to each other at the expense of shrinking the curve. The DSC curve representation automatically maintains a stable length of line segments. This removes the need for the elasticity term, and fairing of the curve can be performed using rigidity alone. That is, unless the length of the interface is also to be minimized.

Curve evolution given by the internal and external forces may trigger a merge, a split, or a disappearance of a phase, but not an insertion of a phase. To allow for a phase insertion, we need to supplement curve evolution with the event of a triangle changing a label. We refer to this operation as *label flip*. In our two-phase segmentation a triangle with a mean pixel intensity I_t is labeled as *inside* if $|I_t - m_{\text{in}}| < |I_t - m_{\text{out}}|$ and *outside* otherwise.

Note that the non-manifold *crossing* points might occur even when using only two phases, consider e.g. the third image in Fig. 1. In our two-phase implementation we do not apply any forces to crossing points, and those are resolved automatically through displacement of the neighbouring points on the interface.

C. Multiphase Segmentation

In multiphase segmentation, triangles are labeled as belonging to a phase $i \in \{1, 2, \ldots N\}$. Interfaces are now line segments dividing two different phases and *triple junction* points generally occur. We still need to define only two actions in order to perform segmentation: the forces on the interface points and the label flip procedure.

Let us first consider the interface points which are neither crossings nor junctions, i.e. the interface points $\mathbf{X}_{ij}$ shared by just two phases i and j. Generalize (5) for any combination of i and j we consider forces with magnitude $(m_{\text{i}} - m_{\text{j}})(I - m_{\text{i}} + I - m_{\text{j}})$, where m_i and m_j denote current mean intensities of the phases i and j. Such external forces would be weaker between phases with mean intensities closer to each other than for two phases with m_i and m_j further apart. As an example, consider the three-phase case illustrated in Fig. 2 *left* with pixel intensities ranging from 0 to 255. Now take two interface points, one between phases 1 and 3 and a second one between phases 2 and 3, but where image data places both points in a region with pixel intensity m_3 (i.e. both points to be included in a phase 3 after deformation). Region forces applied to the first point have a magnitude (denoted f_{13} and drawn green in the illustration) which is a few times larger than a magnitude of forces applied to the second point (f_{23}, blue). Such substantial difference in force magnitudes causes convergence problems, and to avoid these we normalize the region forces. We require force magnitude to take a value of 1 or -1 when the image intensity I exactly equals m_i or m_j. A normalized formulation of the region forces is therefore

$$\mathbf{F}_{\text{ext}}(\mathbf{X}_{ij}) = \frac{I - m_i + I - m_j}{m_i - m_j}\mathbf{N}_{ij}\,. \qquad (6)$$

Here $\mathbf{N}_{ij}$ is a curve normal pointing from the phase i toward the phase j, and with $\mathbf{X}_{ij}$ we indicate that the force is applied only to interface points shared by phases i and j. See Fig. 2 *middle* for how this affects forces in our example, and note that both f_{13} and f_{23} take a value of 1 at m_3.

As for crossings and junctions, we distinguish two situations. When a set of distinct phases meets at a point we call it a *junction-like* point. On the other hand, if a phase is represented more than once around a point, we call it *crossing-like* point. Triple junctions are examples of junction-like points, while the crossing in the third image of Fig. 1 is crossing-like. Under the influence of deforming forces, junction-like points may only move, while resolving forces on crossing-like points might trigger a phase merge or split. In our current implementation, we apply the external forces only to junction-like points and refrain from including active split and merge in our model. Topology changes around crossing-like points are resolved trough displacement of neighbouring interface points.

For junction-like points the external force is a function of the phase contributions. The phase with a mean closest to I should expand most. We decided to retain the contribution of two phases: a phase with the mean intensity immediately smaller than I and the phase with mean intensity immediately

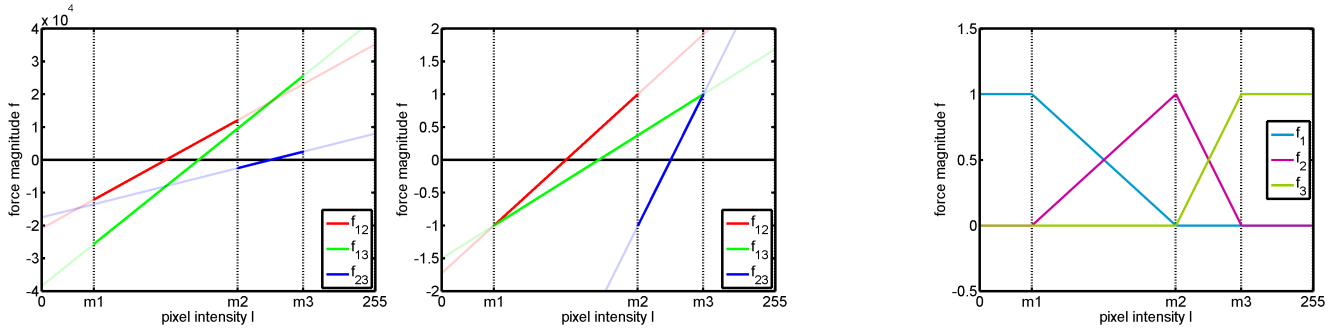

Fig. 2. An illustration showing magnitudes of forces used in three-phase segmentation. The *left* and the *middle* example relate to forces on points shared by two phases $\mathbf{F}_{\text{ext}}(\mathbf{X}_{ij}) = f_{ij}\mathbf{N}_{ij}$. On the *left* are the magnitudes obtained by directly generalizing (5) to three labels, while the *middle* shows the magnitudes after applying our proposed normalization. On the *right*, a force applied to a triple junction shown by a contributions of each phase $\mathbf{F}_{\text{ext}}(\mathbf{X}_{123}) = f_1\mathbf{N}_1 + f_2\mathbf{N}_2 + f_3\mathbf{N}_3$.

larger than I. Those two contributions are linearly weighted. To exemplify the approach, let us consider a triple junction point between regions 1, 2 and 3, and the pixel intensity I which falls between m_1 and m_2. The resulting force would have the contributions from phases 1 and 2 weighed as

$$\mathbf{F}_{\text{ext}}(\mathbf{X}_{123}) = \frac{m_2 - I}{m_2 - m_1}\mathbf{N}_1 + \frac{I - m_1}{m_2 - m_1}\mathbf{N}_2\,, \qquad (7)$$

where $\mathbf{N}_i$ is a curve normal pointing away from the region i. Note that in case of $I = m_i$ the triple junction point moves only in the direction of $\mathbf{N}_i$. Fig. 2 *right* illustrates the weights of the three contributions for any pixel intensity I. Note also that only one contribution remains if I is smaller than the first or larger than the last phase mean value.

The internal forces need also be generalized to include crossings and junctions (distinction is lost here, as internal forces originate from the curve alone). This has been done by tracing the boundaries of each phase and, in the case of a point belonging to more than two phases, averaging the contributions. As a result, the internal forces will try to move the crossing or junction toward the mean of its neighbours.

Finally, we need to consider a label flip. The multiphase case requires a more sophisticated similarity measure than the mean triangle intensity. (Otherwise, a triangle with half of m_1 pixels and half of m_3 pixels might be labeled with 2, provided that means are sorted and somewhat equidistant.) Instead, the following scheme has been implemented. Each pixel of a triangle is assigned to a phase based on the distances $|I - m_i|$. The label of the dominant phase is then assigned to a whole triangle.

IV. Results

Fig. 3 shows an outcome of our four-phase segmentation, when initialized by quadrisecting the dynamic range of the image and labeling the triangles according to their mean intensity. Arguably, the initialization places a curve close to the final solution, but notice the automatic topology changes underway and the correctly resolved junctions. To demonstrate the robustness to initialization and to illustrate curve evolution subject to region forces, we show a segmentation without label flips in Fig. 4. Notice the fully automatic change in topology when the two branches merge.

In Fig. 5, we show the effect of changing the average triangle edge length, which is the only parameter relating to DSC in our current implementation. We can see that details at different scaled have been extracted from the image. A thin gray band appears where the dark and the light intensities blend. Notice also a small boundary artifact present in our current implementation – a triangle edge may not be shorter than a given threshold value, so an object may not come arbitrarily close to the boundary of the image. In Fig. 6 we show a three-phase segmentation of the same image but without label flips. Topology changes and triple junctions are handled fully automatically when two regions meet. Finally, a photograph of Lena segmented into four phases is shown in Fig. 7.

V. Conclusion

Our results confirm that the DSC method can be an interesting addition to an existing toolbox of deformable models used for image processing. We demonstrate the two important qualities of the DSC method, adaptive topology and multiphase support, and show how these properties can be exploited in an image segmentation application. Another advantage of the DSC method, not utilized here, is that the discretization of the space may be exploited. For example, the area or perimeter of the phase can easily be calculated – a useful feature when segmentation is accompanied by quantitative analysis.

We find our initial investigation promising, and are determined to use the DSC method in other segmentation applications. Firstly, we plan to formulate our current approach as a Mumfor Shah [15] model for piecewise constant and piecewise smooth approximation. We also plan segmenting images into an *unknown* number of phases, given some quality threshold for the resulting segmentation/approximation. We are already working on a texture based image segmentation framework which will utilize the DSC method for the curve representation. And finally, we wish to develop a volumetric segmentation based on the DSC method. In that regard, the results shown here are important, since all region-based forces generalize to 3D.

References

[1] C. Xu, A. Yezzi Jr, and J. L. Prince, "On the relationship between parametric and geometric active contours," in *The Asilomar Conference on Signals, Systems,and Computers*, vol. 1. IEEE, 2000, pp. 483–489.

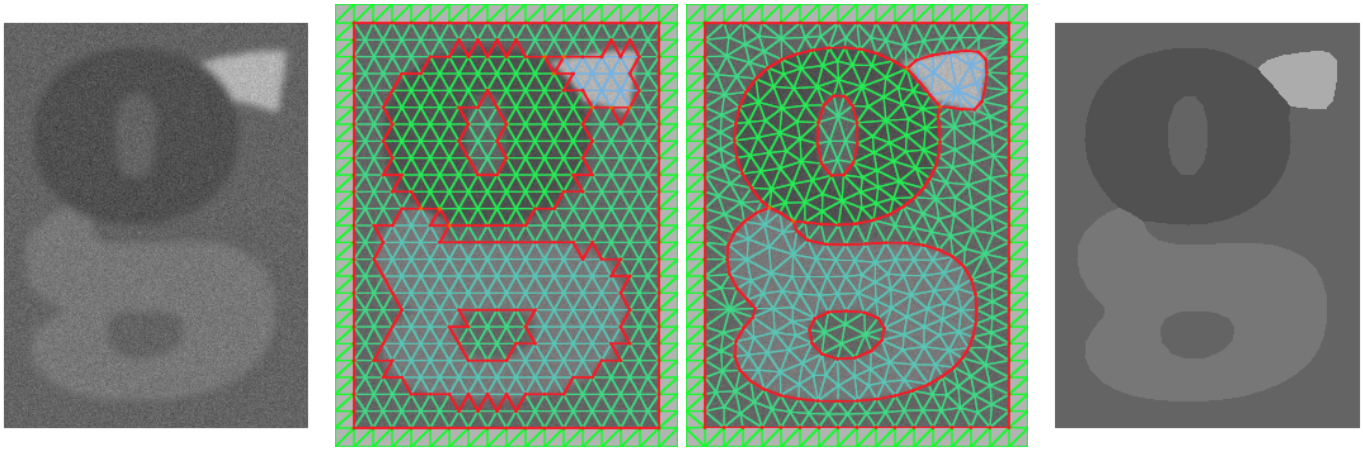

Fig. 3. Segmenting four phases. On the *left* an original image featuring Gaussian noise and smoothed edges. Two images in the *middle* show a configuration after the initial face labeling but before evolving the curve, and a configuration after evolving the curve for 30 iterations. On the *right* a resulting image obtained by filling in each segmented phase with a corresponding mean intensity value.

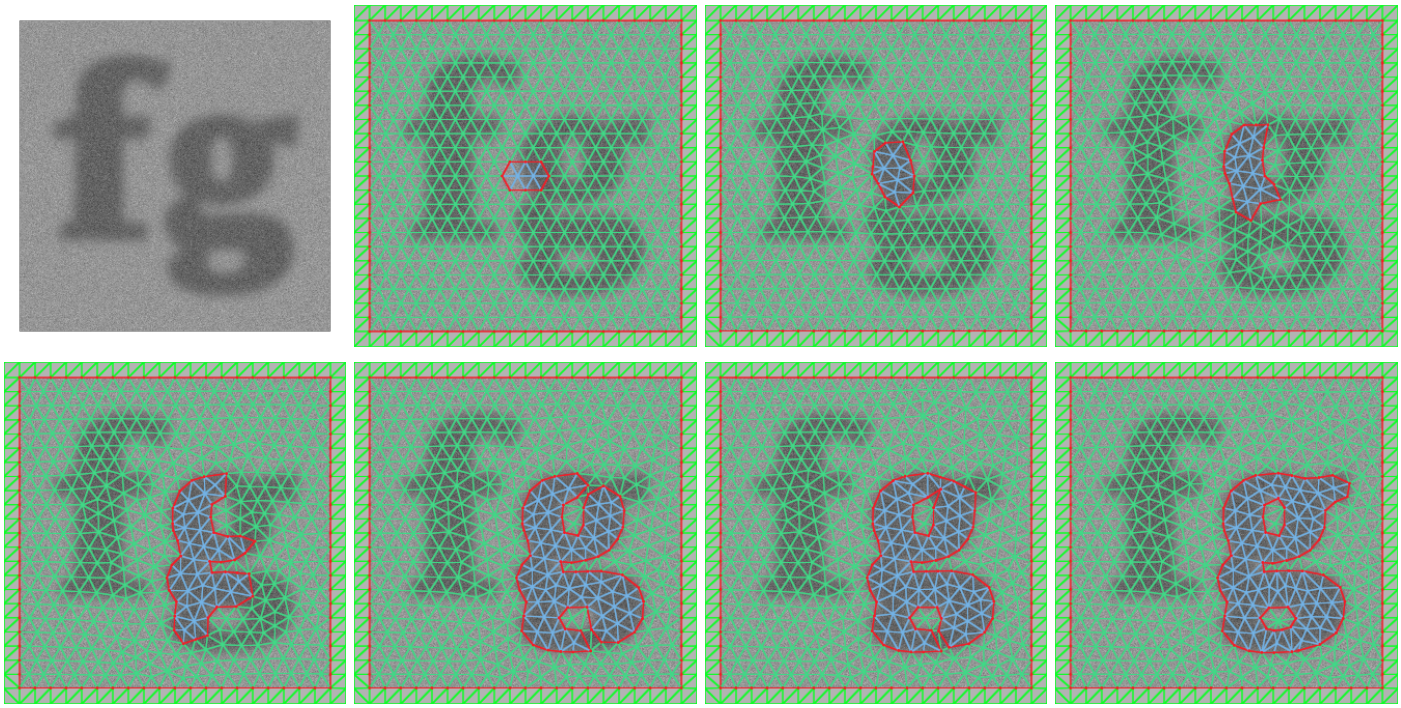

Fig. 4. Segmenting a single contiguous region. In the *upper left* corner an original image featuring Gaussian noise and smoothed edges. Second image in the upper row shows an initial configuration with a few triangles assigned an *inside* label, followed by iterations 3, 9, 28, 43, 45 and 82 of a curve evolution.

[2] M. K. Misztal and J. A. Bærentzen, "Topology-adaptive interface tracking using the deformable simplicial complex," *TOG*, vol. 31, no. 3, p. 24, 2012.

[3] M. K. Misztal, R. Bridson, K. Erleben, J. A. Bærentzen, and F. Anton, "Optimization-based fluid simulation on unstructured meshes," in *VRIPHYS*, 2010, pp. 11–20.

[4] M. K. Misztal, K. Erleben, A. Bargteil, J. Fursund, B. Christensen, J. A. Bærentzen, and R. Bridson, "Multiphase flow of immiscible fluids on unstructured moving meshes," in *Eurographics Symposium on Computer Animation*. Eurographics Association, 2012, pp. 97–106.

[5] A. N. Christiansen, M. Nobel-Jørgensen, N. Aage, O. Sigmund, and J. A. Bærentzen, "Topology optimization using an explicit interface representation," *Structural and Multidisciplinary Optimization*, pp. 1–13, 2013.

[6] M. K. Misztal, J. A. Bærentzen, F. Anton, and S. Markvorsen, "Cut locus construction using deformable simplicial complexes," in *ISVD*. IEEE, 2011, pp. 134–141.

[7] M. Kass, A. Witkin, and D. Terzopoulos, "Snakes: Active contour models," *IJCV*, vol. 1, no. 4, pp. 321–331, 1988.

[8] C. Xu, D. L. Pham, and J. L. Prince, "Image segmentation using deformable models," in *Handbook of Medical Imaging, Volume 2: Medical image processing and analysis*, M. Sonka, J. M. Fitzpatrick, and B. R. Masters, Eds., 2002.

[9] T. McInerney and D. Terzopoulos, "T-snakes: Topology adaptive snakes," *Medical image analysis*, vol. 4, no. 2, pp. 73–91, 2000.

[10] V. Caselles, F. Catté, T. Coll, and F. Dibos, "A geometric model for active contours in image processing," *Numerische mathematik*, vol. 66, no. 1, pp. 1–31, 1993.

[11] R. Malladi, J. A. Sethian, and B. C. Vemuri, "Shape modeling with front propagation: A level set approach," *TPAMI*, vol. 17, no. 2, pp. 158–175, 1995.

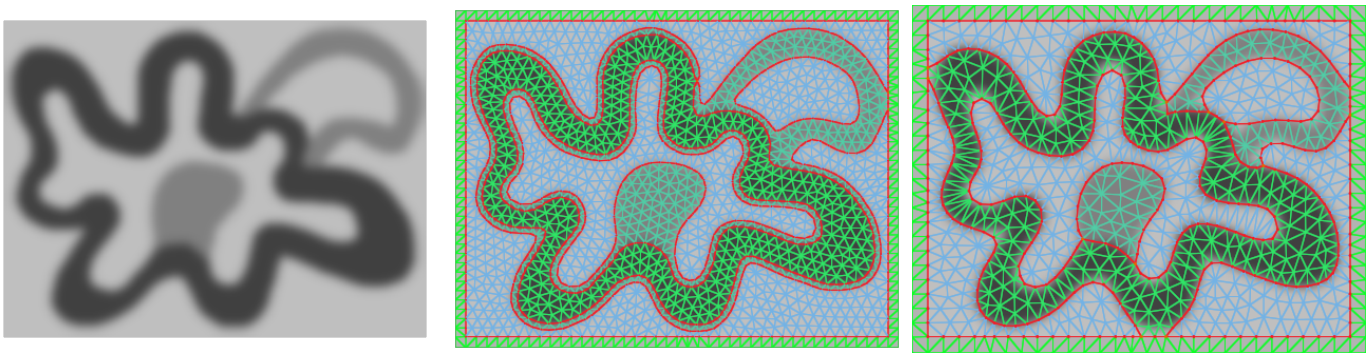

Fig. 5. The effect of the average edge length parameter. On the *left* an original image featuring Gaussian noise and smoothed edges. In the *middle* a segmentation with the average edge length set to 10. For the segmentation on the *right* the average edge length was set to 15.

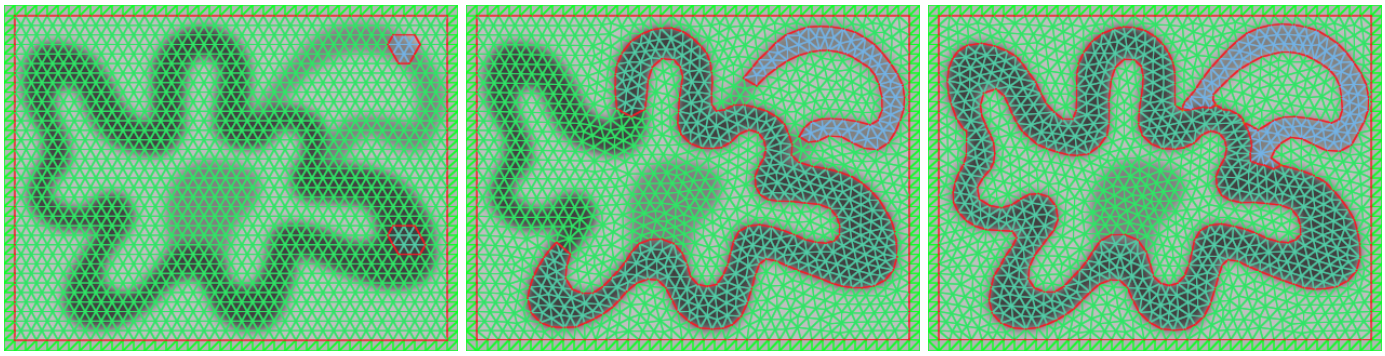

Fig. 6. Segmenting two contiguous regions in a three-phase case. On the *left* a user provided initialization, followed by the iterations 110 and 170 of the curve evolution.

Fig. 7. A four-phase segmentation of Lena with 5 pixels average edge length. On the *left* an original image, followed by the configuration after 30 iterations and the resulting segmentation.

[12] S. Osher and J. A. Sethian, "Fronts propagating with curvature-dependent speed: algorithms based on hamilton-jacobi formulations," *Journal of computational physics*, vol. 79, no. 1, pp. 12–49, 1988.

[13] A. Yezzi Jr, A. Tsai, and A. Willsky, "A statistical approach to snakes for bimodal and trimodal imagery," in *ICCV*, vol. 2. IEEE, 1999, pp. 898–903.

[14] T. F. Chan and L. A. Vese, "Active contours without edges," *TIP*, vol. 10, no. 2, pp. 266–277, 2001.

[15] D. Mumford and J. Shah, "Optimal approximations by piecewise smooth functions and associated variational problems," *Communications on pure and applied mathematics*, vol. 42, no. 5, pp. 577–685, 1989.

[16] H.-K. Zhao, T. Chan, B. Merriman, and S. Osher, "A variational level set approach to multiphase motion," *Journal of computational physics*, vol. 127, no. 1, pp. 179–195, 1996.

[17] A. Tsai, A. Yezzi Jr, and A. S. Willsky, "Curve evolution implementation of the Mumford-Shah functional for image segmentation, denoising, interpolation, and magnification," *TIP*, vol. 10, no. 8, pp. 1169–1186, 2001.

[18] L. A. Vese and T. F. Chan, "A multiphase level set framework for image segmentation using the Mumford and Shah model," *IJCV*, vol. 50, no. 3, pp. 271–293, 2002.